Solid-State Transition of Poly(butylene terephthalate) Induced by Mechanical Deformation

Kohji Tashiro, Yuzo Nakai, Masamichi Kobayashi, and Hiroyuki Tadokoro*

Department of Polymer Science, Faculty of Science, Osaka University, Toyonaka, Osaka, 560 Japan. *Received August 24, 1979*

ABSTRACT: A reversible solid-state transition between α and β forms of poly(butylene terephthalate) [PBT] induced by extension and relaxation of a uniaxially oriented sample has been followed by infrared spectra, differential scanning calorimetry, and small-angle X-ray scattering. By means of quantitative analysis of infrared spectra at room temperature it has been clarified that the molar fraction of the produced β form increases in proportion to the bulk strain and abruptly increases in the vicinity of a certain value of the applied stress corresponding to a plateau in the stress–strain curve. This critical stress of $\alpha \rightleftharpoons \beta$ transition has been found to be a function of temperature. All of these observations have been explained in terms of a first-order phase transition, and the transition phenomena predicted from this mechanism has actually been proved by the measurements of the temperature dependence of infrared spectra under constant stress or strain. The differences in enthalpy and entropy between the α and β forms have been estimated to be $\Delta H = H_\beta - H_\alpha = 5.10$ kJ/mol of monomer unit and $\Delta S = 12.6$ J/K mol of monomer unit, respectively. The length of the plateau in the macroscopic stress–strain curve has been found to increase with an increment of the degree of crystallinity X and the corresponding stress to be almost constant independent of X. The long period measured by small-angle X-ray scattering increases nearly in proportion to the bulk strain and abruptly increases at the critical stress. These experimental results have been interpreted quantitatively by a micromechanical model in which the crystalline and amorphous phases are linked together in series.

Poly(butylene terephthalate) (PBT) transforms reversibly between two crystal phases (α and β) by successive extension and relaxation of oriented samples (Figure 1).[1-10] The macroscopic stress–strain curve of an oriented sample exhibits a characteristic plateau part of constant stress in the strain range of about 4–12%, being quite different from the cases of most synthetic polymers. According to Ward et al.,[2-4] the $\alpha \rightleftharpoons \beta$ crystalline transition induced by tension occurs at this plateau region. In other words, the macroscopic mechanical deformation of the bulk sample is connected directly to the microscopic molecular (or unit cell) deformation in the crystalline region. For most crystalline polymers, the applied stress and the resultant strain of bulk samples do not reflect directly the mechanical deformations in the crystalline parts because of the complicated mixing of the crystalline and amorphous parts. From such a point of view, PBT may be one of the most suitable substances for investigating the roles of crystalline and amorphous phases, separately, on the macroscopic mechanical deformations of polymer materials.

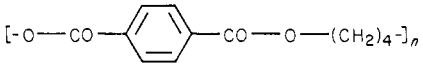

PBT

In the first half of this paper, we will clarify the mechanism of the $\alpha \rightleftharpoons \beta$ solid-state transition by means of quantitative analysis of infrared spectra and also by differential scanning calorimetry performed under tension. The second half of this paper is concerned with the influence of crystallinity on the stress–strain curve and the change of the long period with stress and strain, then a micromechanical model will be proposed.

Experimental Section

Samples and Infrared Spectral Measurements. The samples of PBT used were from a commercial source, Mitsubishi Chemical Industries Co., Ltd. The sample specimens for infrared measurements with thickness of 20 μm were prepared by elongating the unoriented films to about four times the original length in boiling water and subjecting them to heat treatment at 180 °C in vacuo for 4 h under tension.

For the infrared spectral measurement under constant stress or strain the apparatus illustrated in Figure 2 was constructed. This apparatus is designed so as to intensify stress by utilizing a lever and also to control temperature by blowing dried nitrogen (or air) gas, heated or cooled to the desired temperature, upon the clamped film. The infrared spectra were measured by a Japan Spectroscopic Company DS-402G grating infrared spectrophotometer. In Figure 3 the infrared spectra in the region of 1100–700 cm^{-1} measured at room temperature under various strains are reproduced.

Stress–Strain Curves. Stress–strain curves were measured at the same time as the infrared measurements with the apparatus shown in Figure 2. The equilibrium value of strain was measured 15 to 30 min after the application of weights. Annealing effects on the stress–strain curves were examined for the monofilaments (draw ratio 4; heat treated at various temperatures of 80–200 °C) at 20 °C by using an Instron TTDM-type tensile testor and a tensilon Model UTM-III (Toyo Baldwin Co., Ltd.) with a strain rate of 5%/min.

X-ray Measurements. Small-angle X-ray scattering was carried out at room temperature for the samples of the same origins as those used for the stress–strain measurements. The changes of long period with strain were measured by using the sample holder equipped with an elongation device.

The crystallite sizes along the draw direction were estimated according to the Scherrer equation.[11] The X-ray reflection point used is $(\bar{1}04)$, which inclines to the chain axis about 9°[5] and so a correction was made by multiplying by cos ϕ. The integral half width of the reflection was measured using a position-sensitive proportional counter (PSPC) system. The correction of the slit width was made using silicon.

DSC Measurements under Tension. The uniform and highly oriented yarns of 100 μm diameter were submitted to DSC measurements, which were prepared by cold drawing the monofilaments at room temperature followed by heat treatment at various temperatures. The DSC measurements under arbitrary magnitudes of strain were made as follows: One end of the sample is tied to an aluminum rectangular rod (cross section 0.8 × 2.5 mm^2) through a small hole. The yarn is then stretched up to the desired strain by suspending the weight on the other end. After a few minutes, the yarn is wound around the rod carefully, tied securely, and then clamped into the sample pan for DSC measurement. Finely cut samples free from tension were also subjected to DSC measurement for comparison. The heat of fusion was estimated from the thermal analysis curve calibrated with benzoic acid as a standard.

Quantitative Analysis of Infrared Spectra. The vibrational analyses of polarized infrared and Raman spectra of α and β forms will be reported elsewhere.[12] According to these results,[12,13] most bands which change noticeably by mechanical deformation are assigned to the vibrations of the methylene sequences $-O(CH_2)_4O-$. Besides this, these methylene bands disappear for the molten sample and intensify largely as the heat treatment is made, in-

0024-9297/80/2213-0137$01.00/0

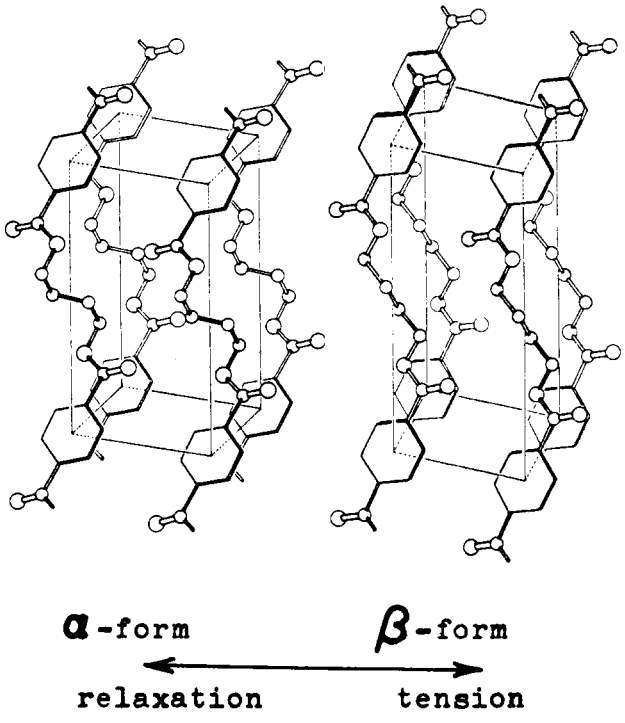

Figure 1. Crystal structures of α and β forms of PBT.[5]

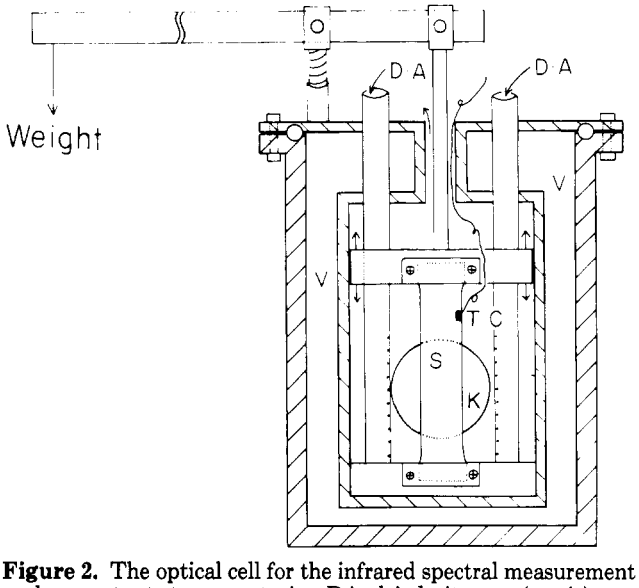

Figure 2. The optical cell for the infrared spectral measurement under constant stress or strain: DA, dried nitrogen (or air) gas; S, sample; K, KBr window; TC, thermocouple; V, vacuum.

dicating that they are from the crystalline region. Therefore we evaluated molar fractions of α and β forms from the infrared intensities of these methylene bands under the assumption of a crystalline two-phase system, ignoring the contribution from the amorphous phase.

The peak intensities were measured by the base line method, and the aromatic ring bands were used as internal standards, whose intensities depend only upon the film thickness d and were measured from the common base line to the methylene bands (e.g., 875 cm^{-1} in Figure 3). According to the methods described in ref 14 and 15, the absorbances D_i of the band i (i = α and β) can be related to each other as follows. Since

$$D_i^r = \frac{D_i}{D(\text{internal standard})} = \frac{\epsilon_i X_i d}{D(\text{internal standard})} = \epsilon_i^r X_i$$

where the superscript r means the reduced value for the internal standard, ϵ_i^r is the molar absorption coefficient, and X_i represents the molar fraction of crystal form i, and since $X_\alpha + X_\beta = 1$,

$$D_\alpha^r = -(\epsilon_\alpha^r/\epsilon_\beta^r)D_\beta^r + \epsilon_\alpha^r \quad (1)$$

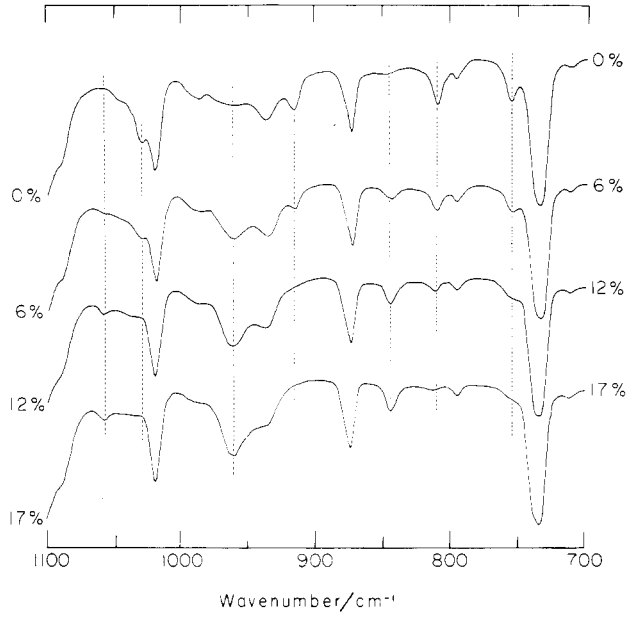

Figure 3. The infrared spectral change of PBT with strain, measured at room temperature.

Table I
Dependence of the Molar Fraction of the β Form upon Stress and Strain Measured at Room Temperature

stress, 10^7 Pa	strain, %	molar fraction of β form (X_β)	stand dev
0	0	0.085	0.045
1.96	0.75	0.108	0.034
3.92	1.87	0.142	0.030
4.92	3.00	0.155	0.032
5.88	4.49	0.205	0.036
6.86	5.99	0.288	0.046
7.84	10.86	0.507	0.021
8.82	11.61	0.541	0.022
9.80	12.73	0.584	0.037
11.76	14.01	0.642	0.048
13.72	16.48	0.674	0.054
9.80	16.48	0.679	0.046
7.84	15.73	0.652	0.045
5.88	11.99	0.493	0.041
3.93	9.74	0.390	0.027
1.96	5.62	0.216	0.028
0	3.75	0.201	0.134

Equation 1 indicates that if we plot D_α^r vs. D_β^r we obtain the linear relationship, the slope giving $(\epsilon_\alpha^r/\epsilon_\beta^r)$. The molar fraction of the β, X_β, for various strain and stress is evaluated from the following equation.

$$X_\beta = \frac{1}{1 + (\epsilon_\beta^r D_\alpha^r/\epsilon_\alpha^r D_\beta^r)} \quad (2)$$

The values of X_β obtained for various band pairs were averaged and tabulated in Table I as a function of strain and stress at room temperature.

Results and Discussion

1. Mechanism of $\alpha \rightleftharpoons \beta$ Transition. Dependence of X_β on Strain and Stress. The strain and stress dependences of X_β are shown in Figures 4 and 5, respectively. In Figure 6 is shown the stress–strain curve, which was measured at the same time as the infrared measurement. These experimental results indicate that (a) X_β increases almost linearly with the increase of strain in the range where the transition goes on, (b) X_β increases abruptly in the vicinity of a certain value of stress (7.5×10^7 Pa), and (c) this stress value corresponds to the plateau region of the stress–strain curve. From all of these results, a–c, the

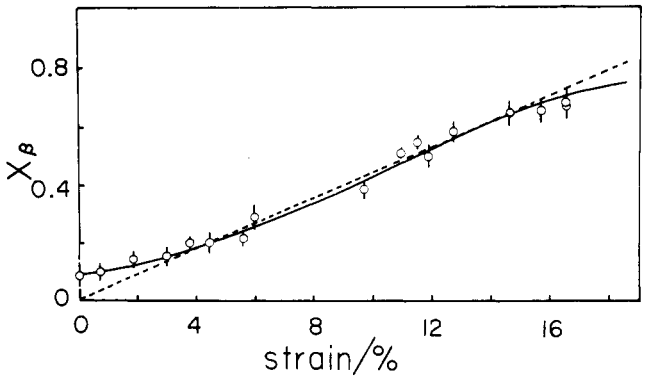

Figure 4. The strain dependence of the molar fraction X_β of the β form.

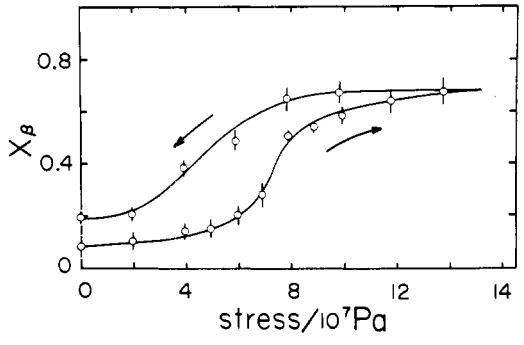

Figure 5. The stress dependence of the molar fraction X_β of the β form.

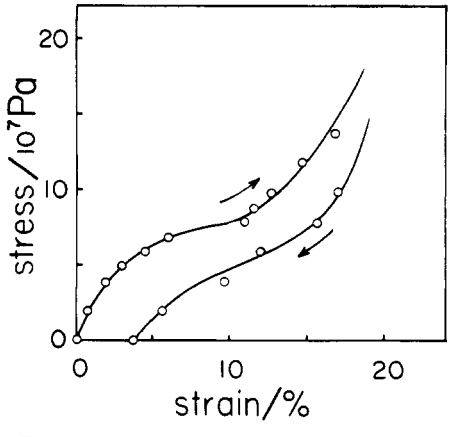

Figure 6. The stress–strain curve measured at the same time as the infrared measurement (room temperature).

$\alpha \rightleftharpoons \beta$ transition is thought to take place at a critical stress and proceed in the plateau region of the stress–strain curve.

Thermodynamical Consideration of $\alpha \rightleftharpoons \beta$ Transition. For the discussion of the mechanism of the phase transition, there are two kinds of theories. One is an equilibrium rate theory.[17,18] According to this theory, the equilibrium is reached at the point where the transition rate of $\alpha \rightarrow \beta$ and that of $\beta \rightarrow \alpha$ is balanced. The relationship between X_i (i = α and β) and load F is given as follows[17,18]

$$\ln (X_\beta/X_\alpha) = (\Delta L/RT)F - \Delta G^*/RT$$

where ΔL is the change in chain length on transition and ΔG^* is the difference in free energy between the α and β forms, respectively. The above equation predicts that X_β is a continuous function of F and that the plot of ln (X_β/X_α) vs. F (or the stress f) gives a straight line. We tried to plot these relations using the experimental data

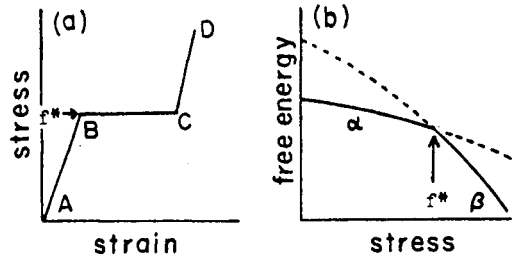

Figure 7. (a) The stress–strain curve and (b) the stress dependence of the free energy of the ideal crystal having the first-order phase transition.

in Table I, but they were not valid at all. Besides, the existence of critical stress, found in the Experimental Section, cannot be predicted by the above equation.

Next, we consider the $\alpha \rightleftharpoons \beta$ transition to be a first-order phase transition. According to the discussion by Ciferri,[19] the first-order phase transition induced by the external stress applied to a crystal should exhibit the following behavior: (i) When the applied stress f does not reach the critical value f^*, only the energetically more stable α form exists (see Figure 7b). The α form is deformed elastically by the stress (line AB in Figure 7a). At the stress f^*, the free energy of the α form, G_α, becomes equal to G_β and the α form transforms into the β form. The bulk strain corresponds to the change of molecular length from the α to the β forms (BC in Figure 7a). When f increases beyond f^*, G_α becomes higher than G_β so that only the β form exists and is deformed by the stress (CD in Figure 7a). (ii) The transition is reversible. (iii) The α and β forms coexist only in the equilibrium state at $f = f^*$. (iv) The strain determines only the relative amount of the α and β forms, that is to say, the relative amount of the β form increases linearly with strain.

The phenomena requested for the first-order phase transition i–iv agree well with the experimental results of a–c described above. Therefore it may be reasonable to recognize the $\alpha \rightleftharpoons \beta$ transition as the first-order solid phase transition.

From the thermodynamic viewpoint of the first-order phase transition, we apply the theory developed by Oth and Flory[20] to this case. When a load F is applied to a one-dimensional crystal with the sides free from any constraint, the free energy change of the system is generally expressed as

$$dG = V\,dP - S\,dT + F\,dL \tag{3}$$

or

$$d(G - FL) = V\,dP - S\,dT - L\,dF \tag{4}$$

where G, S, V, P, T, and L are the Gibbs free energy, entropy, volume, pressure, temperature, and crystallite length along the direction of the applied force, respectively. Total free energy of the system is written as

$$G = X_\alpha G_\alpha + (1 - X_\alpha)G_\beta \tag{5}$$

From the relation $L = X_\alpha L_\alpha + (1 - X_\alpha)L_\beta$ and the equilibrium condition of the system under constant P, T, and F, $[\partial(G - FL)/\partial X_\alpha]_{P,T,F^*} = 0$, we obtain

$$G_\alpha - F^*L_\alpha = G_\beta - F^*L_\beta$$

or

$$d(G_\alpha - F^*L_\alpha) = d(G_\beta - F^*L_\beta)$$

From this equation and eq 4, we obtain

$$[\partial F^*/\partial T]_P = -(\Delta S/\Delta L) \tag{6}$$

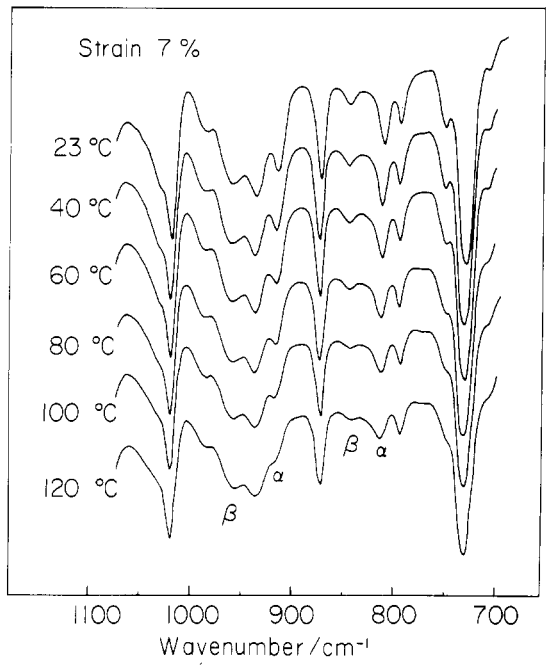

Figure 8. Infrared spectra of PBT measured at various temperatures under a constant strain of 7%.

where $\Delta L = L_\beta - L_\alpha$ and so on. The relationship between the enthalpy and entropy is given as

$$\Delta S = \frac{\Delta H - F^*\Delta L}{T} \tag{7}$$

Thus eq 6 becomes

$$\left[\frac{\partial(F^*/T)}{\partial(1/T)}\right]_P = \frac{\Delta H}{\Delta L} \tag{8}$$

Under the assumption of homogeneous distribution of stress within the sample, the load working on the α crystal is represented as

$$F^* = f^* A_\alpha$$

where f^* is the critical stress applied to the "sample" and A_α is the cross-sectional area of the α crystal, respectively. Therefore, eq 8 is rewritten as

$$\left[\frac{\partial(f^*/T)}{\partial(1/T)}\right]_P = \frac{\Delta H}{A_\alpha \Delta L} \tag{9}$$

Using eq 7 and 9 we can obtain ΔH and ΔS from the temperature dependence of the critical stress f^*.

Now we will examine the temperature dependence of the phase transition under constant strain or stress based on the above consideration.

Phase Transition under Constant Strain. In the case of the first-order phase transition, the molar fractions of the α and β crystals are determined only by the magnitude of the strain. Therefore, the relative amounts of the two forms should be kept constant independent of temperature if the strain remains unchanged. We measured the infrared spectra in the temperature range 20–120 °C under the fixed strain of 7% and also of 12%. Figure 8 shows that the relative intensities of the characteristic bands of the α and β forms hardly change in the temperature range examined, though the reduction of total peak intensities was observed. The experimental results agree well with the above-mentioned prediction.

Temperature Dependence of Critical Stress. At an elevated temperature it is rather difficult to determine

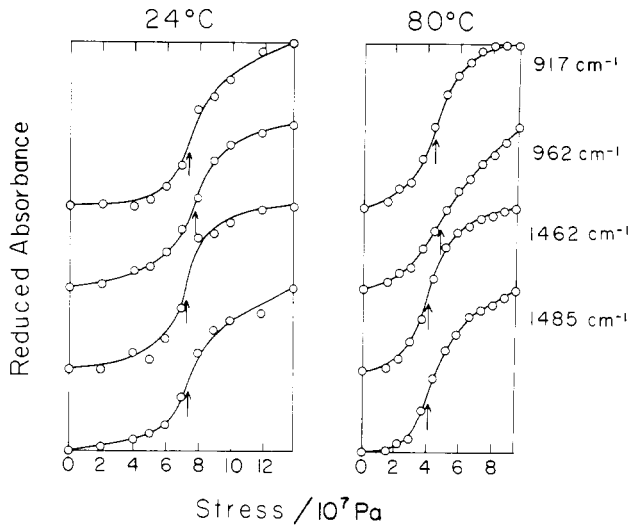

Figure 9. Examples of stress dependence of peak intensities of infrared absorption bands measured at 24 and 80 °C.

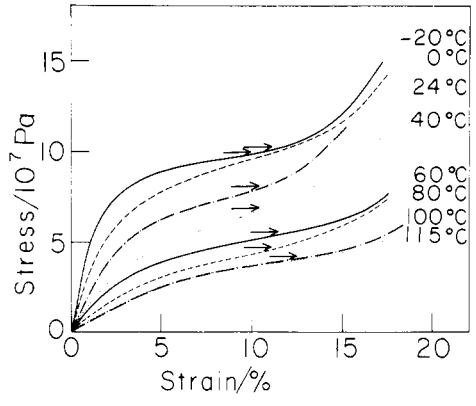

Figure 10. Stress–strain curves at various temperatures measured along with the infrared measurements. The arrows indicate the critical stresses at each temperature obtained from Figure 9 (Table II).

definitely the critical value of stress f^* because the absorptions are, as a whole, broad and therefore the spectral change on transition does not occur as sharply as it does at low temperature. In order to make the infrared intensity change more distinct, the relative absorbances of all of the key bands due to the β form are plotted between zero (before transition) and unity (after completion of transition) as shown in Figure 9. Then the stress corresponding to the steepest change of the reduced intensity was roughly estimated (arrows in Figure 9). The values obtained for various key bands were averaged, giving the critical stress f^* at each temperature. The obtained critical stresses correspond well to the plateau in the stress–strain curves measured at the same temperature as shown in Figure 10. It is, therefore, confirmed that at any temperature the $\alpha \rightleftharpoons \beta$ transition occurs at the stress corresponding to the plateau region of the stress–strain curve. In Table II the critical stresses at various temperatures are given.

Figure 11 shows the plot of f^*/T against $1/T$. In the temperature region–20–60 °C, this plot is linear. The enthalpy and entropy differences between the α and β forms were obtained from the line slope according to eq 7 and 9 with ΔL = 1.36 A and A_α = 22.44 A².[5]

$$\Delta H = H_\beta - H_\alpha = 5.10 \text{ kJ/(mol of monomer unit)}$$

$$\Delta S = S_\beta - S_\alpha = 12.6 \text{ J/(K mol of monomer unit)}$$

From these values the free energy of the α form is calcu-

Table II
Critical Stresses at Various Temperatures

temp, °C	critical stress, 10^7 Pa	stand dev
−20	10.2	0.44
0	9.46	0.50
24	7.48	0.21
40	6.06	0.18
60	5.19	0.38
80	4.26	0.21
100	4.11	0.66
115	3.92	0.57

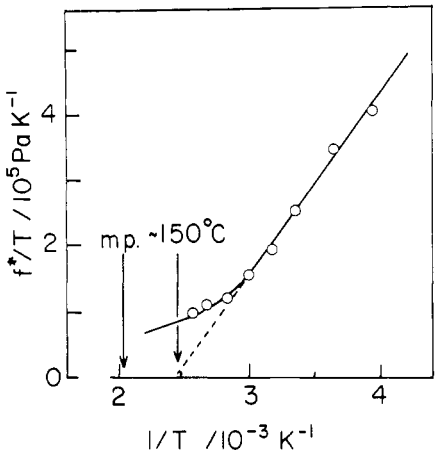

Figure 11. Plot of f^*/T vs. $1/T$.

lated to be lower than that of the β form by about 1.34 kJ/(mol of monomer unit) at room temperature. The β form cannot be obtained until the applied stress does not exceed this free-energy gap.

The f^*/T vs. $1/T$ plot in Figure 11 deviates from the linear relation at higher temperatures. If ΔH and ΔS are kept unaltered through the whole temperature range, the $\alpha \rightleftharpoons \beta$ transition is expected to occur under free tension at about 150 °C, which is the extrapolated point of the straight line to $f^*/T = 0$ in Figure 11. However, this prediction has not yet been confirmed experimentally by means of infrared measurements at high temperatures and of the DSC measurements. Because of a very small linear thermal expansion coefficient along the chain direction due to the covalent bondings of the skeletal atoms, ΔL may be kept constant throughout the whole temperature range concerned. Therefore, the deviation from the straight line may be due to the lowering of ΔH and ΔS from the values determined above.

$\alpha \rightleftharpoons \beta$ Transition under Constant Stress. Figure 12, which exhibits the temperature dependence of the critical stress f^*, shows that if we measure the infrared spectra with changing temperature under a certain constant stress, the $\alpha \rightleftharpoons \beta$ transition should occur at such a temperature that the applied stress equals the critical value. Actually the infrared spectra showed an abrupt change from the α form to the β form at 70 °C under the constant stress of 4.6×10^7 Pa, coinciding with the prediction from Figure 12.

It should be noted here that when the temperature is lowered again down to room temperature under the same constant stress, the β form does not return to the α form. The α form does not appear until the stress is released. This may be due to freezing-in of the metastable state on lowering of the temperature. In connection with this phenomenon, we found that the cold drawn PBT sample gives the X-ray and infrared patterns characteristic of the β form, although the crystallinity is not as high. But heating of the sample above 40 °C (T_g) brings it into the

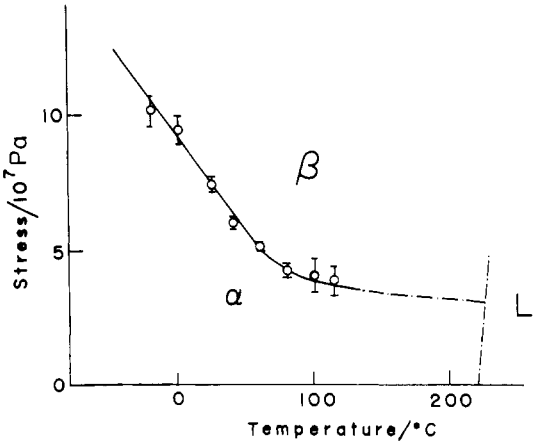

Figure 12. Temperature dependence of the critical stress f^*. L indicates the liquid phase.

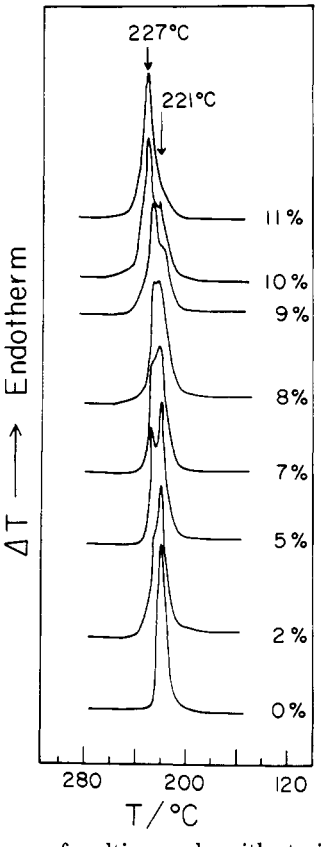

Figure 13. Change of melting peaks with strain (indicated in the figure). The heating rate is 10 °C/min.

α form under no tension or into the well-crystallized β form under tension which reverts to the α form with relaxation. In the experiments of Figures 5 and 6, an appreciable amount of β form remains when the sample is relaxed after the β form is generated by stretching, so called hysteresis. The flexibility of such a sample is very low and returns to the original flexible state with heating. All of these phenomena are due to the "residual strain" generated after the repetition of extension and relaxation of the sample (Figure 5). It should not be overlooked that the apparent "irreducibility" of the transformation caused by the residual strain appreciably affects the mechanical property of PBT samples.

DSC Measurements under Tension. Because of the difference in melting point between α and β forms due to the difference in crystal structures, the DSC peaks are predicted to change with the strain. Figure 13 shows the

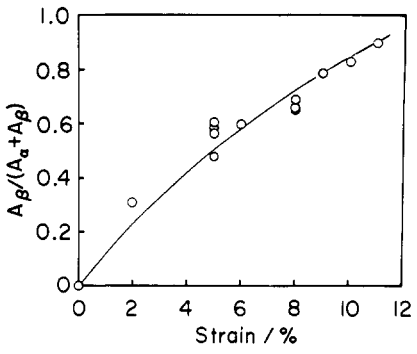

Figure 14. The strain dependence of the ratio of the areas of the two peaks shown in Figure 13.

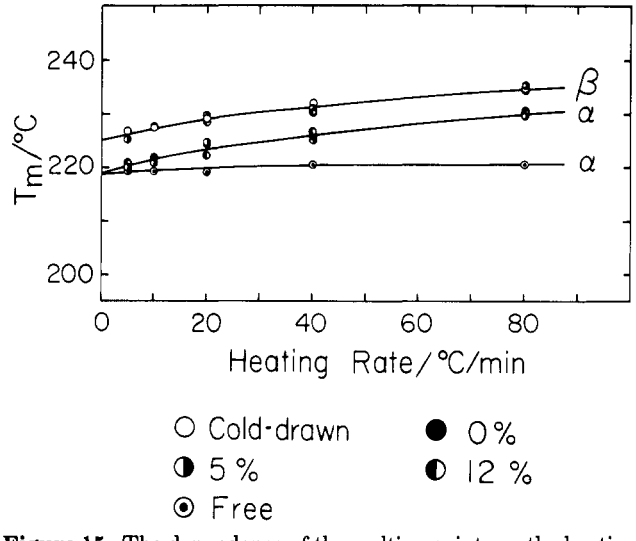

Figure 15. The dependence of the melting points on the heating rate: (○) cold-drawn sample restrained in the DSC sample pan; (●, ◑, ◐) samples strained at 0, 5, and 12%, respectively; (◉) sample measured under free tension.

change of melting peaks measured under the various strains for the cold-drawn samples annealed at 130 °C for 3 h under tension. From this figure we can find that the peak at the higher temperature side enlarges with the increase of strain. The ratio of areas under the two peaks is nearly proportional to the strain as shown in Figure 14, which corresponds well to the observed relationship between X_β and strain in Figure 4. On the measurements of DSC under tension, however, the upward shift of melting point, i.e., the phenomenon of superheating, is frequently observed for the ordinary polymers such as polyethylene and poly(ethylene terephthalate).[21-23] The higher temperature peak observed here might be from such a phenomenon. Then we examined the dependence of melting peaks on the heating rate under the various conditions as shown in Figure 15. Two curves which correspond to the two peaks appearing under finite heating rate are extrapolated to each respective value (225 °C for the high-temperature peak and 219 °C for the low-temperature peak) at zero heating rate. These facts show that the lower peak is from the melting of α crystals and the higher one from the melting of β crystals.

The enthalpies and entropies of fusion for almost pure α and β forms are obtained as follows.

$$\Delta H_\alpha \simeq \Delta H_\beta \simeq 9.20 \text{ kJ/(mol of monomer unit)}$$

$$\Delta S_\alpha \simeq 18.7 \text{ J/(K mol of monomer unit)}$$

$$\Delta S_\beta \simeq 18.5 \text{ J/(K mol of monomer unit)}$$

According to Conix and Kerpel,[24] $\Delta H°$ is 31.80 kJ/(mol of monomer unit) for the degree of crystallinity of 100%. Then the degree of crystallinity of the sample used here is estimated as about 30%, in good agreement with the result of the density method described later.

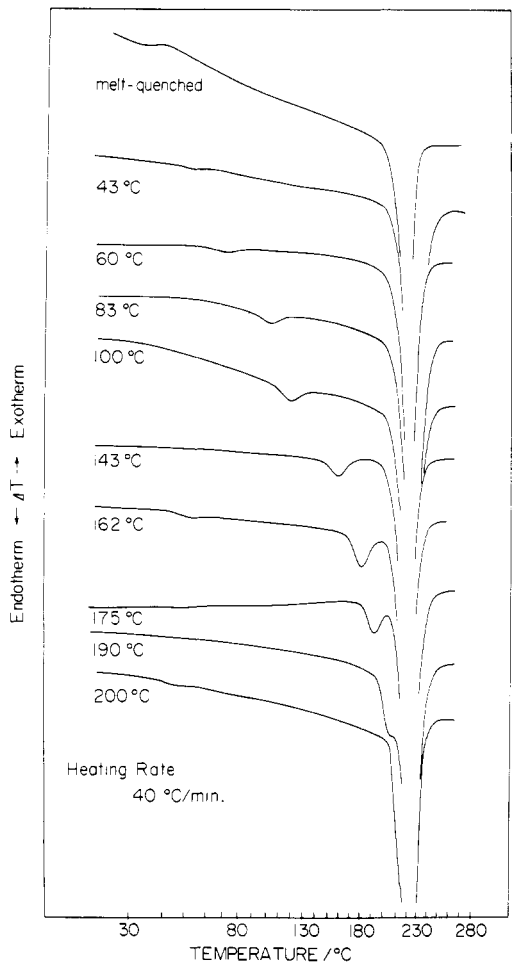

Figure 16. DSC diagrams of PBT melt-quenched samples annealed at various temperatures, measured under free tension.

In the preceding section we predicted that the $\alpha \rightleftharpoons \beta$ transition should occur under free tension at the temperature of about 150 °C and the endothermic peak should appear at this temperature in the DSC thermograph because the enthalpy increases on the transition from α to β phases. The sample annealed at 130 °C, for example, gave the small peak at about 130 °C in the DSC diagram when measured under free tension. But this peak shifted to the higher temperature side as the annealing temperature was raised, and the position almost coincides with the annealing temperature itself as shown in Figure 16. This subpeak is ultimately united with the main melting peak. Therefore the peak is considered to be due to the melting of imperfect crystal and not to the $\alpha \rightleftharpoons \beta$ phase transition under free tension.

2. Micromechanical Model of PBT. In the above discussion it has been assumed that the macroscopic deformation of the PBT sample directly corresponds to that of the crystalline region. We must, however, investigate in more detail whether this assumption is reasonable or not. For this purpose the effects of the crystallinity and of the fine structure on the phase transition will be dealt with in this section.

Small-Angle X-ray Measurements. Annealed PBT monofilaments show a meridional two-point pattern of small-angle X-ray scattering. As the c dimension (unit cell) increases on the $\alpha \rightleftharpoons \beta$ transition,[5] the long period should

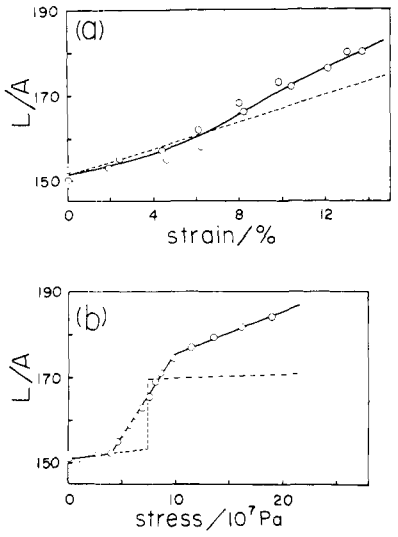

Figure 17. The change of the long period with (a) strain and (b) stress: (—) observed results; (- - -) calculated results for the sample with the degree of crystallinity X ($=L_{cry}/L$) of 80%.

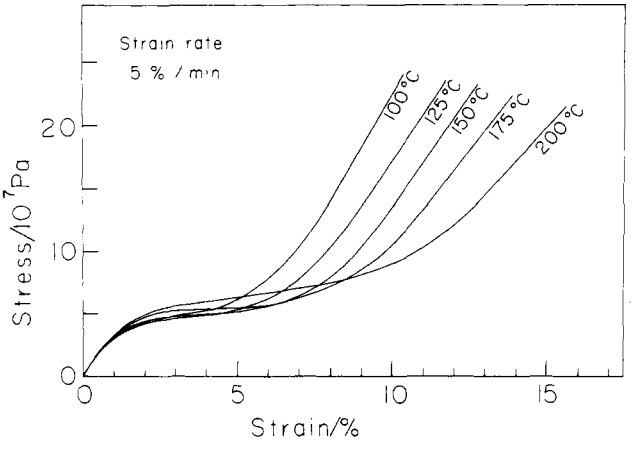

Figure 18. Stress–strain curves of PBT monofilaments annealed at various temperatures for 1 h.

also change with it. Figure 17a,b shows the dependence of long period on the strain and stress, respectively, measured at room temperature. The long period increases approximately in proportion to the strain. It abruptly increases in the vicinity of the critical stress, although the change is not as sharp because an inhomogeneous distribution of stress is likely as stated in the previous section (Figure 6). This behavior is common to all samples with different degrees of crystallinity.

Effect of Crystallinity on the Stress–Strain Curve. In Figure 18 the stress–strain curves of uniaxially oriented samples annealed at the various temperatures are shown. As the annealing temperature is raised, the lengths of the plateaus increase remarkably. The values of the strains at the starting and terminal points of the plateau are plotted against the annealing temperature in Figure 19. The definitions of the starting (A) and the terminal (B) points are shown in this figure. Although it is not shown in this figure, the degree of crystallinity estimated by the density measurement increases linearly with annealing temperature (about 10% at 80 °C to 36% at 200 °C) when the density of the melt-quenched sample was adopted as that of the amorphous state. The stress at the plateau region in Figure 18 is nearly constant irrespective of the degree of crystallinity. The strain at the terminal point of the plateau shifts toward the larger value as annealing temperature or degree of crystallinity increase, while the

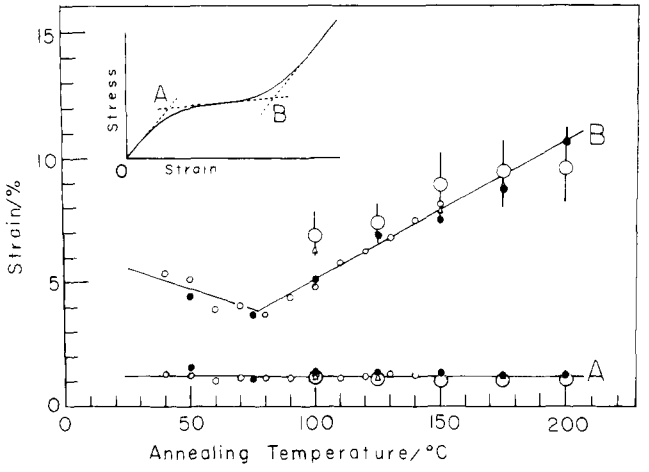

Figure 19. Dependence of the plateau length upon the annealing temperature: (○) samples drawn at room temperature (drawing rate 2 cm/min); (△) samples drawn at 80 °C (2 cm/min); (●) samples drawn quickly by hand at room temperature; (◯) calculated values (see text).

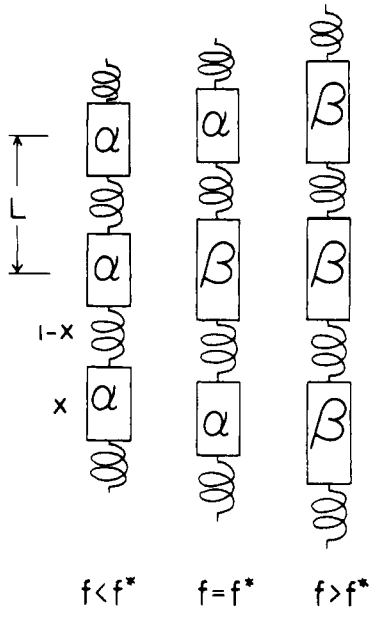

Figure 20. Series model of PBT.

strain at the starting point of the plateau remains constant. Various samples of different sources (draw temperature, etc.) give essentially the same results as the above case as shown in Figure 19.

The reason for the lowering of the initial strain A for the annealing temperatures of 40–70 °C in Figure 19 is not clear at the present.

Series Model. The experimental results shown in Figures 17, 18, and 19 reasonably suggest a series model of crystalline and amorphous regions as a micromechanical model of PBT sample because the model should lead to an increase of plateau length in the stress–strain curve with the increase of crystallinity. In the case of a parallel model, on the contrary, the terminal point of the plateau would be constant independent of the degree of crystallinity.

Then we predicted the effects of crystallinity on the stress–strain curve and also on the long period based on the series model (Figure 20) and made a comparison with the observed results. (i) For the applied stress f below the critical stress f^*, the crystal and amorphous regions are deformed elastically. The effect of elongation velocity on the stress–strain curves is found to be largely negligible

at room temperature which is below T_g. Therefore we can ignore the effect of viscosity as an approximation and we treat the amorphous phase as a purely elastic body. Furthermore we assumed that the amorphous phase does not crystallize during elongation. Then for $0 \leq f < f^*$,

$$\sigma = \sigma_\alpha + \sigma_{am} = \frac{f}{E_\alpha} X + \frac{f}{E_{am}}(1 - X) \quad (10)$$

$$L = L_0(1 + \sigma) = L_0\left[1 + f\left(\frac{X}{E_\alpha} + \frac{1 - X}{E_{am}}\right)\right] \quad (11)$$

where X is the ratio of crystallite size to the long period L_0 (Figure 20), σ is the bulk strain, and E_α and E_{am} are Young's moduli of the α form and of the amorphous phase, respectively. (ii) When the stress f becomes equal to the critical stress f^*, the $\alpha \rightleftharpoons \beta$ phase transition takes place in the crystalline region and the crystallite size increases. The length of the amorphous region is kept constant because the stress remains unchanged during the phase transition. At the terminal point of the phase transition, we express the sizes of the crystalline and amorphous phases as follows.

$$L^*_{cry} = XL_0(1 + 0.117) \quad (12)$$

$$L^*_{am} = (1 - X)L_0(1 + f^*/E_{am}) \quad (13)$$

Here the α crystal transforms into the β form with the extension of 11.7%. Using these equations, we found the strain σ^* and the long period L^* at the terminal point of transition to be

$$\sigma^* = \frac{(L^*_{cry} + L^*_{am}) - L_0}{L_0} = 1.117X + (1 - X)\left(1 + \frac{f^*}{E_{am}}\right) - 1 \quad (14)$$

$$L^* = L^*_{cry} + L^*_{am} = L_0\left[1.117X + (1 - X)\left(1 + \frac{f^*}{E_{am}}\right)\right] \quad (15)$$

(iii) When the stress f is beyond the critical stress f^*, the elastic deformations of the β form and amorphous phase take place again. For $f > f^*$,

$$f = f^* + \frac{\sigma - \sigma^*}{\frac{X}{E_\beta} + \frac{1 - X}{E_{am}}} \quad (16)$$

$$L = L^*_{cry}\left(1 + \frac{f - f^*}{E_\beta}\right) + (1 - X)L_0\left(1 + \frac{f}{E_{am}}\right) = L_0\left[1.117X\left(1 + \frac{f - f^*}{E_\beta}\right) + (1 - X)\left(1 + \frac{f}{E_{am}}\right)\right] \quad (17)$$

The theoretical stress–strain curves and the dependence of long period on the stress and strain can be calculated for the degree of crystallinity X by using eq 10–17. The used parameters are as follows: Young's moduli of α and β forms, E_α and E_β, are the theoretical values of 10.1 and 26.9 GPa, respectively, calculated for the single chains, the used force constants being taken from ref 25. [Recently Nakamae et al.[26] measured the Young's moduli of them along the chain direction by the X-ray method to be about 8.7 and 20.4 GPa, respectively, coinciding well with the calculated values.] The Young's modulus of the amorphous region is assumed to be 3.9 GPa, the observed value for the unannealed and unoriented sample. For the critical stress f^*, the value of 7.48×10^7 GPa in Table II is used. The initial long period L_0 is 151 A. The calculated results of stress–strain curves are shown in Figure 21, reproducing the observed curves shown in Figure 18.

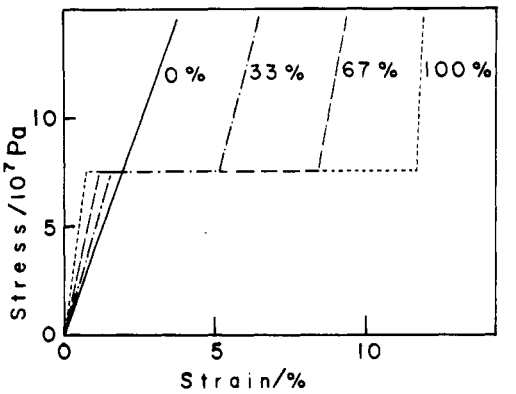

Figure 21. Stress–strain curves for various crystallinities calculated based on the series model shown in Figure 20.

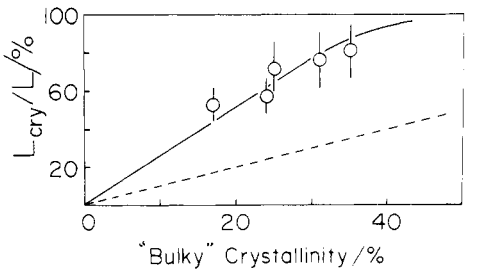

Figure 22. Relationship between L_{cry}/L estimated by X-ray measurements and "bulk" crystallinity estimated by density measurements.

For the quantitative comparison of the observed values of starting and terminal points of the plateau (Figure 19) with the calculated ones, we should notice that the degree of crystallinity X defined in the above equations is not the "bulk" crystallinity estimated by the density measurement but the ratio of (crystallite size)/(long period) along the draw direction. Figure 22 shows the relationship between the two kinds of degree of crystallinity, that is L_{cry}/L and the bulk crystallinity $(\rho - \rho_{am})/(\rho_{cry} - \rho_{am})$ where ρ is the specific volume of the sample. The averages of two values, estimated from the assumption of band profile of X-ray reflection as Gaussian-type and Cauchy-type,[11] are used for the crystallite size L_{cry}. Figure 22 indicates that the ratio L_{cry}/L is much larger than the value estimated from the density measurement, in other words, the ratio (crystallite size)/(amorphous length) along the draw direction is different from those in other directions. In fact, the calculation using the "bulk" crystallinity as X leads to the appreciably smaller values of strain at the terminal point of the plateau and also of the change of long period with stress. In Figure 19 are plotted the starting and terminal strains of the plateau calculated by using the observed values of L_{cry}/L, giving a fairly good agreement with the observed results.

In Figure 17 is compared the calculated stress dependence of the long period with the observed one for the sample with the ratio of L_{cry}/L = ca. 80%. Although the change of long period is qualitatively reproduced by the calculation, the observed long period deforms more than the theoretical one as the strain and stress increase. Especially Figure 17a shows that above the terminal point of the $\alpha \rightleftharpoons \beta$ phase transition the long period deviates from the linear line indicating the same behavior of the macroscopic strain as that of the long period. Such a deviation has also been observed for some other polymers.[27] The

reason may be understood to be the reduction of homogeneity of polymer deformation after the formation of submicrocracks in a stressed sample, that is some regions in the polymer are highly stretched and some regions are only weakly stretched. In the present case, too, such a heterogeneous stretching might occur detectably after approaching completion of the $\alpha \rightleftharpoons \beta$ phase transition.

Fibers such as PBT, keratin,[19] and rubber,[20] in which the reversible phase transition is induced by the reciprocation motion of successive extension and relaxation of the samples, can become a material with excellent mechanical properties such as high fatigue resistance because the strain energy added to the sample is consumed by the phase transition and a kind of cushion thus generated can keep the sample against the direct mechanical rupture. It may be important to develop such polymer materials.

Acknowledgment. The authors are grateful to Mitsubishi Chemical Industries Co., Ltd., for supplying the samples of PBT. They also wish to express their gratitude to Mr. Shin-ichi Ishikawa of the Infrared Spectroscopy Section, Faculty of Science, Osaka University, for his production of the optical cell for the infrared spectral measurements under constant stress and strain.

References and Notes

(1) C. A. Biye, Jr., and J. R. Overton, *Bull. Am. Phys., Ser. 2*, **19**, 352 (1974).
(2) R. Jakeways, I. M. Ward, M. A. Wilding, I. H. Hall, I. J. Desborough, and M. G. Pass, *J. Polym. Sci., Polym. Phys. Ed.*, **13**, 799 (1975).
(3) I. M. Ward, M. A. Wilding, and H. Brondy, *J. Polym. Sci., Polym. Phys. Ed.*, **14**, 263 (1976).
(4) R. Jakeways, T. Smith, I. M. Ward, and M. A. Wilding, *J. Polym. Sci., Polym. Lett. Ed.*, **14**, 41 (1976).
(5) M. Yokouchi, Y. Sakakibara, Y. Chatani, H. Tadokoro, T. Tanaka, and K. Yoda, *Macromolecules*, **9**, 266 (1976).
(6) Z. Mencik, *J. Polym. Sci., Polym. Phys. Ed.*, **13**, 2173 (1975).
(7) I. H. Hall and M. G. Pass, *Polymer*, **17**, 807 (1976).
(8) I. J. Desborough and I. H. Hall, *Polymer*, **18**, 825 (1977).
(9) I. M. Ward and M. A. Wilding, *Polymer*, **18**, 327 (1977).
(10) M. G. Breseton, G. R. Davies, R. Jakeways, and I. M. Ward, *Polymer*, **19**, 17 (1978).
(11) L. E. Alexander, "X-ray Diffraction Methods in Polymer Science", Wiley-Interscience, New York, 1969.
(12) K. Tashiro, Y. Nakai, M. Kobayashi, and H. Tadokoro, to be published.
(13) I. M. Ward and M. A. Wilding, *Polymer*, **18**, 327 (1977).
(14) K. O. Hartman, G. L. Carlson, R. E. Witkonski, and W. G. Fateley, *Spectrochim. Acta, Part A*, **24**, 157 (1968).
(15) M. Okazaki, I. Hara, and T. Fuziyama, *J. Phys. Chem.*, **80**, 64 (1976).
(16) Ward and Wilding[13] assigned the 812 cm^{-1} band to the amorphous gauche band. But this band intensifies with the heat treatment, i.e., the crystallization sensitive band, and shows the remarkably infrared polarization property. Furthermore this band disappears with extension of the sample. Thus it should be assigned to the vibrational mode [$r(CH_2)$] of the α crystalline phase.
(17) M. Feughelman, *J. Appl. Sci.*, **10**, 1937 (1966).
(18) H. Burte and G. Halsey, *Textile Res. J.*, **17**, 465 (1947).
(19) A. Ciferri, *Trans. Faraday Soc.*, **59**, 562 (1963).
(20) J. F. M. Oth and P. J. Flory, *J. Am. Chem. Soc.*, **80**, 1297 (1958).
(21) A. Miyagi and B. Wunderlich, *J. Polym. Sci., Part A-2*, 1401 (1972).
(22) S. B. Clough, *J. Macromol. Sci. Phys.*, **4**, 199 (1970).
(23) M. Todoki and T. Kawaguchi, *J. Polym. Sci., Polym. Phys. Ed.*, **15**, 1507 (1977).
(24) A. Conix and R. van Kerpel, *J. Polym. Sci.*, **40**, 521 (1959).
(25) K. Tashiro, M. Kobayashi, and H. Tadokoro, *Macromolecules*, **10**, 413 (1977).
(26) K. Nakamae, M. Kameyama, and T. Matsumoto, private communication.
(27) V. S. Kuksenko and A. I. Slutsker, *J. Macromol. Sci. Phys.*, **12**, 487 (1976).

Energy Migration and Transfer in Molecularly Doped Polymers

G. E. Johnson

Webster Research Center, Xerox Corporation, Webster, New York 14580.
Received October 2, 1979

ABSTRACT: The migration and transfer of singlet excitation in polystyrene films doped with *N*-isopropylcarbazole as an energy donor has been investigated. Fluorescence decay measurements on these molecularly doped polymer films in the presence of two types of energy acceptor, dimethylterephthalate and perylene, are used to determine the mechanism for singlet migration among the donor subsystem of like chromophores. The donor concentration dependence of the fluorescence quenching process is found to be consistent with a mechanism in which the singlet excitation migrates by a series of random walk steps with each step involving a Förster dipole–dipole resonance transfer. Excitation diffusion lengths as a function of the donor concentration have been determined and shown to extrapolate in the limit of high concentration to a value close to that for poly(*N*-vinylcarbazole).

The migration of electronic excitation in organic molecular crystals is a photophysical process which has been extensively investigated over a period of many years.[2a] Perhaps the most dramatic evidence for this process is revealed in spectroscopic studies where it is generally observed that the fluorescence spectrum of the host crystal is dominated by fluorescence from unwanted impurities or by fluorescence from small concentrations of purposely added guest molecules.[3] More recently a variety of experiments have been carried out which lead to a greatly increased understanding of the dynamic aspects of the exciton migration process and of the nature of the various excited state interactions which can occur in these systems.[4] Emission spectroscopic techniques, both steady state and time resolved, have also been utilized to investigate the wealth of photophysical processes which occur in organic polymers.[5] The stimuli for the ever increasing body of literature concerning the photophysics of polymers can perhaps be considered to cover a somewhat broader spectrum than those which led to the vast literature on molecular crystals. While surely there is great interest in the photophysics of polymer systems from a purely scientific point of view, polymers are certainly of more technological importance than molecular crystals. For example, the ability to render stability to synthetic polymers by the addition of dopants is in many cases the result

0024-9297/80/2213-0145$01.00/0